Breakdown of Energy Equipartition in Vibro-Fluidized Granular Media in Micro-Gravity

2012 Chinese Phys. Lett. 29 074501

(http://iopscience.iop.org/0256-307X/29/7/074501)

CHIN. PHYS. LETT. Vol. 29, No. 7 (2012) 074501 Express Letter

Breakdown of Energy Equipartition in Vibro-Fluidized Granular Media in Micro-Gravity *

CHEN Yan-Pei(陈延佩)[1,2], Pierre Evesque[2], HOU Mei-Ying(厚美瑛)[1**]

[1]*Key Laboratory of Soft Matter Physics, Beijing National Laboratory for Condensed Matter Physics, Institute of Physics, Chinese Academy of Sciences, Beijing 100190*

[2]*Lab MSSMat, Ecole Centrale de Paris, UMR 8579 CNRS, 92295 Châtenay-Malabry Cedex, France*

(Received 20 June 2012 and accepted by LIN Zong-Han)

We present a micro-gravity experimental study of intermediate number density vibro-fluidized inelastic spheres in a rectangular container. Local velocity distributions are investigated, and are found to deviate measurably from a symmetric distribution for the velocity component of the vibrating direction when dividing particles along the vibration direction into several bins. This feature does not exist in the molecular gas. We further study the hydrodynamic profiles of pressures p and temperatures T in positive and negative components, such as p_y^+ and p_y^- and T_y^+ and T_y^-, in accordance with the sign of velocity components of the vibrating direction. Along vibration direction, granular media are found to be not only inhomogeneous and anisotropic, but also different greatly in positive and negative components. Energy equipartition breaks down in this case.

PACS: 45.70.−n, 51.30.+i, 51.10.+y DOI: 10.1088/0256-307X/29/7/074501

Granular media have caught much of physicists' attention in theoretical, simulation and experimental studies in recent years. They are deemed as ideal model systems for studying the statistical and dynamical properties of nonlinear, non-equilibrium and dissipative systems. Yet no satisfactory theory exists. Granular systems are treated by resembling the molecular gas or ordinary fluids[1] in many works although great differences are found between them.[2] For a nearly homogeneous granular system, it is assumed that the granular systems follow the Maxwell–Boltzmann velocity distribution $e^{-mv^2/2kT}$ and conform to equipartition of energy. From the Maxwell–Boltzmann distribution, temperature is defined as $T = m\langle v^2\rangle/2$ $(k = 1)$ when there is no macroscopic flow in the system. However, an increasing number of works point out that the non-Gaussian velocity distribution[3−12] appears in granular gases. The profile deviates from the Maxwell distribution as can be seen from the overpopulation in the high-velocity tail. Kinetic reasons of these deviations are still unclear. Among all the potential reasons, concerns on the driving mechanism[2,7,13−16] have been raised. Brey *et al.*[16] discussed discontinuity effects by the direct Monte Carlo simulation of the sawtooth vibration boundary due to the particle-number conservation near the boundary. Local distribution functions f near the boundary walls are found to be asymmetric and discontinuous. Herbst *et al.*[2] also found the same asymmetric velocity distributions f in simulation. However, they did not indicate whether this asymmetry and discontinuity due to the boundary effect only exist in the 'boundary layer' or extends to the whole cell. If it extends to the whole cell, it will lead in turn to the following question: how does it vary in terms of the distance from the boundary? As mentioned in Ref. [17], Navier–Stokes order hydrodynamics is not sufficient for describing moderately inelastic steady-state vibrated systems. Further investigation, especially in experiment, is needed.

In this Letter, we report our experimental observations obtained in Airbus of *Novespace* (2006 Campaign) in a 2D vibro-fluidized granular system. This experiment was developed by CNES and performed in collaboration with Yves Garrabos' group. In the experiment, the particle velocity distributions are obtained in both x and y directions globally and locally. It is found that the probability distributions of velocities both along parallel (v_y) and perpendicular (v_x) to the vibration direction are exponential and symmetric, when taking into account all the particles. However, when the particles are divided into different bins along the vibration direction, the local velocity distribution of (v_y) is found to deviate measurably from a symmetric one. Considering that the distributions of local velocities are asymmetric, we measure hydrodynamic profiles for positive and negative components in accordance with the sign of velocity components. It is found that these two components, positive and negative, of p_y, n_y and T_y differ not only at the boundary layer but also in the whole cell. Besides the extensive boundary effect, particles are found to be inhomoge-

*Supported by the Knowledge Innovation Project of the Chinese Academy of Sciences under Grant No KJCX2-YW-L08, the National Natural Science Foundation of China under Grant No 10720101074 and 11034010, the Special Fund for Earthquake Research of China under Grant No 201208011, and CNRS, CNES Special Funds.

**Corresponding author. Email: mayhou@aphy.iphy.ac.cn

neous and granular temperature anisotropic.

Firstly, we present the experimental method. Then we show that the local velocity distributions are asymmetric in the y direction. Finally, local hydrodynamic parameters are investigated.

In our experiment a quasi-2D quadrate cell (side walls in aluminum, front and back walls in glass, $V = 10\,\text{mm} \times 10\,\text{mm} \times 1.4\,\text{mm}$) containing 47 bronze spheres is driven in the y direction by a sinusoidal oscillating shaker. A snapshot is shown in Fig. 1. The diameter of the bronze spheres is $1.21\,\text{mm} \pm 0.02\,\text{mm}$, and the area fraction is 0.54. The spheres can rotate in three dimensions but only have two-dimensional translational motion.

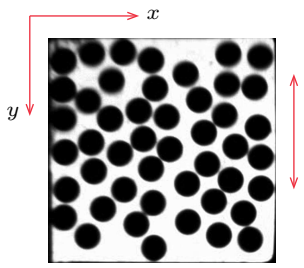

Fig. 1. Snapshot of the cell particles. The cell contains 47 bronze sphere particles, driven in the y direction at various vibration parameters (A, V_ω, Γ, f). The diameter of particle is 1.21 mm and cell size is ($10\,\text{mm} \times 10\,\text{mm} \times 1.4\,\text{mm}$). The cell is divided into 7 bins along the y direction.

The cell is fixed on a V455 LDS shaker, which vibrates in the y direction. The vibration controller is the same as those in previous works.[9,18] The movement of the beads is recorded by a fast camera (499 frames per second). The light emitting diodes (LEDs) are mounted in the reverse side of the cell to increase the contrast between beads and the background. The experiments are performed for 30 parabolic flights in a two-hour Campaign. Each parabolic flight has about 20 s for micro-gravity ($0.0g \pm 0.05g$ with g being the gravitational constant). Within the 20 s of each parabolic flight only one second is recorded by the fast camera. The resolution of the cell image is $288\,\text{pixel} \times 288\,\text{pixel}$ ($1\,\text{pixel} = 0.035\,\text{mm}$). The frequency range in the experiment is from 40 Hz to 130 Hz, the oscillating amplitude ranges from 0.005 to 0.912 mm, and the corresponding acceleration is in the range of $0.1g$ to $9g$. In this study, we only present four sets of data under different vibrating conditions. We use notations (A, V_ω, Γ, f) to represent amplitude, vibrating peak velocity, acceleration and frequency, respectively.

All the parameters are determined by image analysis using the software ImageJ. Images recorded by the fast camera are firstly processed to get the positions of the bead center, which are calculated through the ultimate eroded points (UEPs) in the Euclidian distance map (EDM). Afterwards, particles are tracked using the program of the minimum-distance algorithm. Since our system has moderate number density, the spheres can not move extensively, the minimum-distance algorithm can work well in our case. The magnitude of accuracy obtained in this way reaches 0.01 mm.

Next, we discuss local velocity distributions with the vibration parameters ($A = 0.23\,\text{mm}$, $V_\omega = 0.07\,\text{m/s}$, $\Gamma = 21.56\,\text{m/s}^2$, $f = 49\,\text{Hz}$). The particle velocities are obtained from 499 image sequences within 1 s. Considering the anisotropy of the vibration, we analyze x and y components of velocity distributions separately. Furthermore, in order to understand the spatial profiles of velocities, the local velocity distributions are investigated. The cell is divided into 7 bins along the y axis, and the distributions of velocity v_x and v_y are averaged in each bin. The velocity is scaled by the maximum driving velocity V_ω (0.07 m/s).

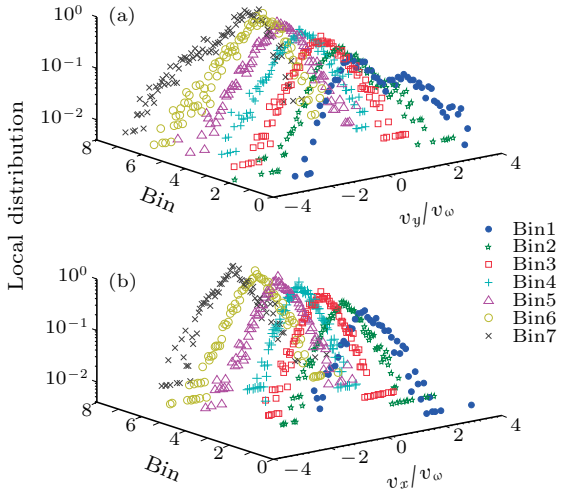

Fig. 2. Local distribution functions of (a) v_y and (b) v_x on log-linear scales. There are 7 bins along the vibration direction y. The vibration parameters ($A = 0.23\,\text{mm}$, $V_\omega = 0.07\,\text{m/s}$, $\Gamma = 21.56\,\text{m/s}^2$, $f = 49\,\text{Hz}$)

As shown in Fig. 2, the local velocity distribution of v_y (Fig. 2(a)) is asymmetric for each bin in the y direction, while the distribution of v_x (Fig. 2(b)) in each bin remains symmetric. Two peaks appear in local velocity distribution profiles of v_y in bins near two heating boundaries $\widetilde{y} = 0$ or 1 ($\widetilde{y} = y/L$). Remarkable asymmetry in local profiles are observed. While moving away from the driving wall, asymmetry of the profile of the local velocity distribution v_y becomes less profound. In the box center, the profile becomes symmetric, where the boundaries effect may be balanced out.

For a quantitative analysis of asymmetry, momenta technique of statistics is adopted. Skewness S, i.e. the third standardized moment, is calculated for each local velocity distribution. The result is shown in Fig. 3. The skewness of variable q with n sample

points is defined as

$$S = \frac{\frac{1}{n}\sum_{n}^{i=1}(q_i - \bar{q})^3}{[\frac{1}{n}\sum_{n}^{i=1}(q_i - \bar{q})^2]^{3/2}}, \tag{1}$$

where $\bar{q}$ is the average over all n sample points q_i. Figure 3 compares the skewness of profiles for v_x and v_y in different bins along the y axis. The skewness changes linearly from positive to negative, and is around zero at the center of the box for v_y profiles, while skewness seems flat for local v_x distribution in these seven bins.

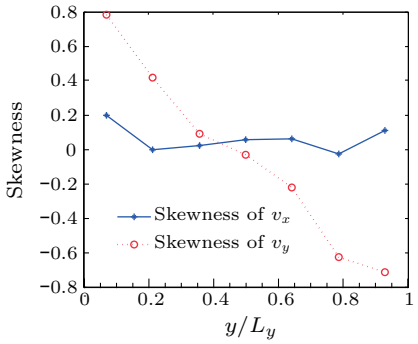

Fig. 3. The skewness of v_x and v_y distribution profiles along y/L_y (see Eq. (1)).

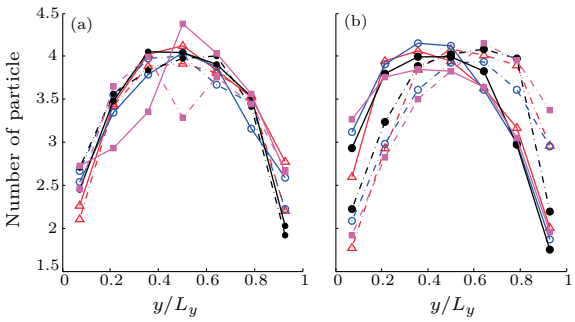

Fig. 4. (a) The number of particles in each bin with velocity $v_x^{\pm}$. (b) The number of particles in each bin with velocity $v_y^{\pm}$. Triangle: $V_\omega = 0.07\,\mathrm{m/s}$. Open circle: $V_\omega = 0.067\,\mathrm{m/s}$. Closed circle: $V_\omega = 0.087\,\mathrm{m/s}$. Closed square: $V_\omega = 0.038\,\mathrm{m/s}$. Solid curves are for the positive component, and the dashed curves for the negative ones.

In the steady state, conservation of momentum requires[16]

$$\int_0^{+\infty} v f(v) dv = -\int_{-\infty}^{0} v f(v) dv. \tag{2}$$

In turn, near the boundary $y = 0$, the number of particles moving towards the wall and leaving the wall shall be conserved, that is, the number of particles leaving the vibrating wall shall be equal to the number of particles moving towards the vibrating wall in a sawtooth excitation:

$$f_y^-(v_y)v_y = f_y^+(2V_\omega - v_y)(v_y - 2V_\omega). \tag{3}$$

Here f_y^+ (f_y^-) is the velocity distribution function for the $v_y > 0$ ($v_y < 0$). The number density n near the boundary $y = 0$ can therefore be obtained from the particle-number conservation mentioned above,[16]

$$n_y = 2n_y^- + 2V_\omega \int \frac{f_y^-}{v_y - 2V_\omega} dv_y. \tag{4}$$

It implies that at the boundary $y = 0$, n_y^+ is smaller than n_y^-. The discrepancies between n^+ and n^- can be confirmed in our experimental results shown in Fig. 4.

The Navier–Stokes-like hydrodynamic equations are used to describe mass, momentum and energy of the granular system. The local pressure, temperature and number density in terms of field are established. On basis of the above asymmetric velocity distribution, the local hydrodynamic field is analyzed in two components based on the sign of the velocity component.

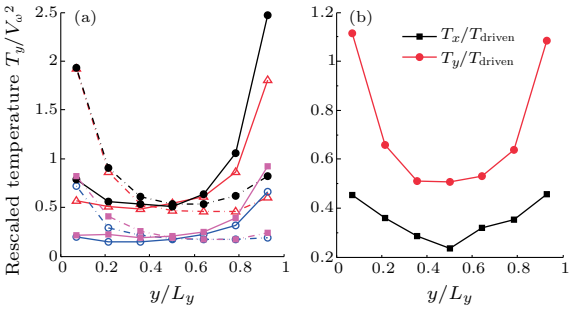

Fig. 5. Experimental results of temperature profiles in terms of positions. (a) The scaled temperature $T_y^{\pm}(y)$ with velocity $v_y^{\pm}$. Triangle: $V_\omega = 0.07\,\mathrm{m/s}$. Open circle: $V_\omega = 0.067\,\mathrm{m/s}$. Closed circle: $V_\omega = 0.087\,\mathrm{m/s}$. Closed square: $V_\omega = 0.038\,\mathrm{m/s}$. Solid curves are for the positive component, and the dashed curves for the negative ones. (b) The two components of temperature T_x and T_y under the vibration condition for $V_\omega = 0.07\,\mathrm{m/s}$.

Starting from the measured particle positions (x, y), particle velocities can be obtained and separated into four parts: $v_x^+(v_x > 0)$, v_x^- $(v_x < 0)$, v_y^+ $(v_y > 0)$, and v_y^- $(v_y < 0)$. Hydrodynamic parameters p_x^+ (p_y^+), p_x^- (p_y^-), n_x^+ (n_y^+), n_x^- (n_y^-), T_x^+ (T_y^+), T_x^- (T_y^-) can then be derived. The notation $p_x^+(y)$ in each bin along the y direction is defined as $p_x^+(y) = \sum(v_x^+)^2(y)$. The mass of the particles is assumed to be unitary, $m = 1$. The temperature $T_x^+(y) = p_x^+(y)/n_x^+ k_B$ is scaled by the $T_{\mathrm{drive}} = V_\omega^2$, and V_ω is the peak value of the vibrating velocity. Here k_B is set to 1. Same definition can be applied to $T_x^-(y)$, $T_y^+(y)$, $T_y^-(y)$, and $T_x(y) = (n_x^+(y)T_x^+(y) + n_x^-(y)T_x^-(y))/(n_x^+(y) + n_x^-(y))$, $T_y(y) = (n_y^+(y)T_y^+(y) + n_y^-(y)T_y^-(y))/(n_y^+(y) + n_y^-(y))$. The energy equipartition requires that $T_x^+(y)$ equals $T_x^-(y)$ and $T_y^+(y)$ equals $T_y^-(y)$. Our experimental results (Fig. 5), however, indicate the breakdown of energy equipartition in vibro-fluidized granular media.

The four components of the number density $n_x^+(y)$, $n_x^-(y)$, $n_y^+(y)$, $n_y^-(y)$ are shown in Figs. 4(a) and 4(b). The notation of $n_x^+(y)$ means the spatial profile of

the number density of particles with velocity $v_x > 0$ along the y direction. It is observed that $n_x^+(y)$ and $n_x^-(y)$ overlap and peak at the cell center as shown in Fig. 4(a). The curves in Fig. 4(b) confirm the difference between $n_y^+(y)$ and $n_y^-(y)$ near the boundaries, predicted by Eq. (4). Moreover, n_y^+ and n_y^- do not overlap. The components $n_y^+(y)$ and $n_y^-(y)$ are mirror symmetric to each other as shown in Fig. 4(b). It is apparent that $n_y^+(y) \neq n_y^-(y)$. This was often ignored in previous works when calculating the transport parameters in granular system.[1,19]

Although the temperature anisotropy in vibro-fluid granular systems has been studied by computer simulation in recent years,[2,20–23] experimental investigation has not been reported so far. In our experimental study, we observe that $T_x^+(y) \approx T_x^-(y)$, and $T_x^+(y)(T_x^-(y))$ are symmetric with the central axis of the cell (it is not shown here), but $T_y^+(y)$ (or $T_y^-(y)$) along the y axis is asymmetric (Fig. 5(a)). The values of $T_y^+(y)$ (or $T_y^-(y)$) are larger than those of $T_x^+(y)$ $(T_x^-(y))$. $T_y^+(y)$ $(T_y^-(y))$ is greater near the boundary at $y = 0$ $(y = L)$ as shown in Fig. 5(a). Temperature anisotropy is apparent (Fig. 5(b)), and the two components T_y^+ and T_y^- are mirror symmetric with each other. The temperature anisotropy is discussed in Ref. [23]. The non-isotropic driving of a granular gas in a steady state is the necessary cause of anisotropy of the granular temperature.

The objective of this work is to provide an experimental study of the boundary effect in vibro-fluidized granular gas system. We have studied the velocity distribution in the vibration direction locally and globally. The velocity distribution is found anisotropic, and both the x and y components are non-Gaussian. We measure the local velocity distribution along the vibration direction and find that the v_x distributions are still symmetric, while the distributions profile v_y becomes asymmetric, and even double-peaked near boundaries. The skewness of the profiles is found linear along y with S=0 at the cell center. This implies that boundary effects are extensive. The particle number density is found not a constant and peaked at the center of the cell. The hydrodynamic parameter profiles $p_x^+(y)$ and $p_x^-(y)$, $T_x^+(y)$ and $T_x^-(y)$, $n_x^+(y)$ and $n_x^-(y)$ under different vibration strengths are found to be overlapped, but the $p_y^+(y)$ and $p_y^-(y)$, $n_y^+(y)$ and $n_y^-(y)$, $T_y^+(y)$ and $T_y^-(y)$ are mirror symmetric to each other.

In summary, the temperature is found to follow (i) $T_x \neq T_y$ (anisotropic) and (ii) $T_y^+ \neq T_y^-$. Point (ii) links with the asymmetric local velocity distribution. This imposes $T_y^+(y) \neq T_y^-(y)$ in such a system. The asymmetry in the y component profiles can be understood as the dissipation of the energy input through collision with the boundary walls and energy transformed to the x component through particle collisions. Energy equipartition is broken down in this case. This suggests that further investigations of hydrodynamic description of such vibro-fluidized granular systems are needed. A local equation of state different from the global one, if it exists, shall be carefully examined and derived.

References

[1] Grossman E L, Zhou T and Ben-Naim E 1997 *Phys. Rev.* E **55** 4200
[2] Herbst O, Müller P, Otto M and Zippelius A 2004 *Phys. Rev.* E **70** 051313
[3] Sergei E E and Pöchel T 1997 *J. Stat. Phys.* **86** 1385
[4] Olafsen J S and Urbach J S 1999 *Phys. Rev.* E **60** R2468
[5] Olafsen J S and Urbach J S 1998 *Phys. Rev. Lett.* **81** 4369
[6] Rouyer F and Menon N F 2000 *Phys. Rev. Lett.* **85** 3676
[7] Kudrolli A, Wolpert M and Gollub J P 1997 *Phys. Rev. Lett.* **78** 1383
[8] Losert W, Cooper W D G, Delour J, Kudrolli A and Gollub J P 1999 *Chaos* **9** 682
[9] Hou M, Liu R, Zhai G, Sun Z and Lu K 2008 *Micrograv. Sci. Technol.* **20** 73
[10] Noije T P C and Ernst M H 1998 *Granul. Matter* **1** 57
[11] Brey J J, Ruiz-Montero M J and Cubero D 1996 *Phys. Rev.* E **54** 3664
[12] Huthmann M, Orza J A and Brito R 2000 *Granul. Matter* **2** 189
[13] Evesque P 2002 *Poudres Grains* **13** 20
Evesque P 2002 *Poudres Grains* **13** 40
[14] Evesque P 2005 *Poudres Grains* **15** 1
Evesque P 2005 *Poudres Grains* **15** 18
[15] Liu R, Hou M and Evesque P 2009 *Poudres Grains* **17** 1
[16] Brey J J, Ruiz-Montero M J and Moreno F 2000 *Phys. Rev.* E **62** 5339
[17] Herbst O, Muller P and Zippelius A 2005 *Phys. Rev.* E **72** 041303
[18] Leconte M, Garrabos Y, Palencia F, Lecoutre C, Evesque P and Beysens D 2006 *Appl. Phys. Lett.* **89** 243518
[19] Brilliantov N V and Pöschel T 2004 *Kinetic Theory of Granular Gases* (New York: Oxford University)
[20] Brey J J and Cubero D 1998 *Phys. Rev.* E **57** 2019
[21] Barrat A and Trizac E 2002 *Phys. Rev.* E **66** 051303
[22] McNamara S and Luding S 1998 *Phys. Rev.* E **58** 813
[23] van der Meer D and Reimann P 2006 *Europhys. Lett.* **74** 384